Arid Zone Journal of Engineering, Technology and Environment. August, 2010; Vol. 7, 44 -58

Print ISSN: 1596-2490, Electronic ISSN: 2545-5818
www.azojete.com.ng

ANALYSIS OF PRESSURE DROP AND EFFECTIVENESS IN MICRO CROSS-FLOW HEAT EXCHANGER

Garba, I.[1]

Abstract

A theoretical model that predicts the thermal and fluidic characteristics of a micro cross-flow heat exchanger is developed in this study. The theoretical model is validated by comparing the theoretical solutions with the experimental data from the literature. This model describes the interactive effect between the effectiveness and pressure drop in the micro heat exchanger. The analytical results show that the average temperature of the hot and cold side flow significantly affects the heat transfer rate and the pressure drop at the same effectiveness. Different effectiveness has a great influence upon the heat transfer rate and pressure drop. When the micro heat exchanger material is changed from silicon to copper, the thermal conductivity changes from 148 to 400 W/mK. The heat exchanger efficiency is also similar. Furthermore, the dimensions effect has a great influence upon the relationship between the heat transfer rate and pressure drop. Therefore, the methodology presented in this paper can be used to design a micro cross-flow heat exchanger.

1. Introduction

The development of micro heat exchangers began with solving the heat dissipation problem in high-speed integrated circuits. Now this technology can be applied in the field of small volume, high heat flux devices such as electrical component cooling, aerospace industry and biochemistry. The idea of using micro channel for the cooling of very large-scale integration (VLSI) was first proposed by Tuckerman (1984). He used anisotropic etching and precision mechanical sawing techniques to manufacture 280 lm deep micro channels in 500 lm thick (11 0) oriented silicon wafers. He reported on a direct contact and cold plate hybrid technology using laminar water flow in the micro-passages and absorbing a heat flux of 150 W/m². Micro channels for heat exchange interfaces were thereby established. From the investigation of heat transfer and heat exchanger, the narrow and deep channel, like a heat sink has a very high heat transfer rate. The higher aspect ratio channels have higher heat transfer effects. Friedrich and Kang (1994) fabricated micro channels on metal foil using diamond machining techniques. The channel cross-area shape can be fabricated as a trapezoid, rectangle or triangle. The metal foils are then bonded together using diffusion bonding into a micro cross-flow heat exchanger. The total heat transfer rate can reach 300 MW/m² K. They used basic heat transfer and fluid flow equations to establish heat exchanger models with constant hot and cold flow side temperatures. They effectively predicted the Reynolds number on the cold flow side. Studies of conventional compact heat exchanger design theories were already completed by Kays and London (2004).

Kang *et al.* (2002) fabricated micro channels with 9000 lm lengths, 40 µm widths and 200 µm depths on (110) silicon wafers using MEMS technology. Wafers with hundreds of high aspect ratio channels were bonded together using diffusion bonding with aluminium as the medium layers. The core of the micro heat exchanger was about 0.918 cm^3, and the density of the heat transfer area was 15294 kg/m^3. Using pure water as the working fluid, the Reynolds number showed that the fluid field always exhibited a laminar flow. The heat transfer measured

[1] Department of Mechanical Engineering, Bayero University, Kano. Nigeria

between the hot and cold fluid was 5 kW, and the overall heat transfer coefficient reached 24.7kW/m²K.

This study used heat transfer and fluid flow equations to establish a plate-type cross-flow micro heat exchanger model based on the micro heat exchanger dimensions made by Kang *et al.* (2002) to verify with the theoretical and experimental results. It analyzed the interactive effect between the effectiveness and the pressure drop in the micro channels. The results from this study can be used for design calculation on micro heat exchangers.

2. Materials and methods

The theoretical model in this paper is based on the cross flow heat exchanger. The channel shape of the hot and the cold flow is rectangular. A schematic of the structure is illustrated in Figure 1. It shows the heat exchanger arrangement with dimensions of *X*, *Y*, and *Z*. The channels have a width of *c* and a depth of *b*, and are separated by a fin thickness of *d*. The thickness of the channel bottom plate is *a*. The core dimensions show the volume where the two fluid streams flow pass each other and do not include any volume taken up by manifolds, etc.

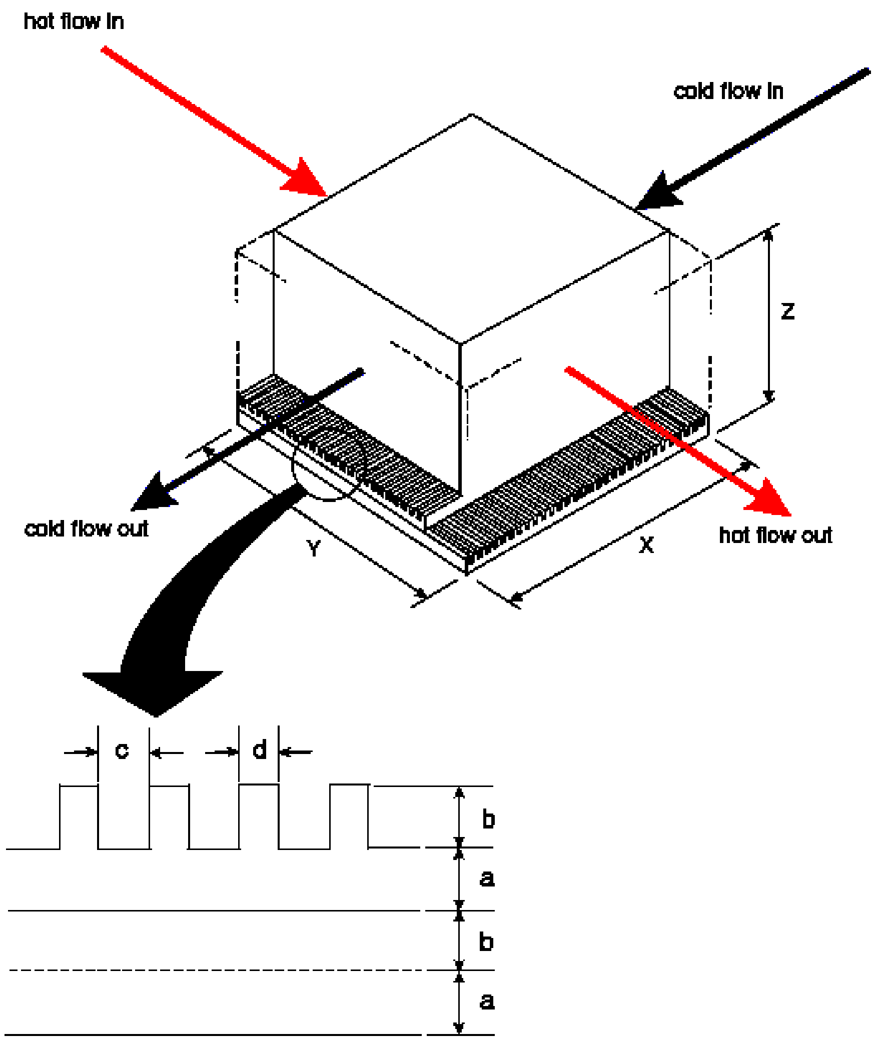

Fig. 1. Plate-type cross-flow micro heat exchanger.

The first portion of the procedure involves determining the two ratios. The first ratio is the total heat transfer area on one side of the exchanger to the total volume of the exchanger. The second ratio is the total heat transfer area on one side of the exchanger to the volume between the plates on that side *b*, expressed as:

$$\alpha_1 = \frac{b\beta_1}{2b+2a} \tag{1}$$

$$\alpha_2 = \frac{b\beta_2}{2b+2a} \tag{2}$$

and

$$\beta_1 = \frac{N_1 \times [(2b+2c)\times Y]}{XYZ \times \dfrac{b}{2b+2a}} \tag{3}$$

$$\beta_2 = \frac{N_2 \times [(2b+2c)\times Y]}{XYZ \times \dfrac{b}{2b+2a}}$$

Where; subscript 1 refers to the hotter fluid and its associated heat transfer surface.
Subscript 2 refers to the colder fluid and its heat transfer surface.
N is the total number of channels on one side.

The top and bottom surface areas of the heat exchanger are very small, so the effect of radiation and natural convection can be negligible. Some simplifying assumptions are required before building the theoretical model. The major assumptions are:

(1) The fluid flow is laminar.
(2) The fluid flow is incompressible and steady.
(3) Constant solid and fluid properties.
(4) Heat transfer rate is steady.
(5) Negligible radiation heat transfer.
(6) Negligible natural convective heat transfer.

Because the volume of the heat exchanger is very small, the temperature distribution of the exchanger is almost the same. Then it can be assumed that the wall of the heat exchanger has a constant surface temperature, and the fluid flow is a fully developed laminar flow, depicted in the following (Equation 5);

$$Nu_T = 7.541 \times \left[1 - 2.61 \times \left(\frac{c}{b}\right) + 4.97 \times \left(\frac{c}{b}\right)^2 - 5.119 \times \left(\frac{c}{b}\right)^3 + 2.702 \times \left(\frac{c}{b}\right)^4 - 0.548 \times \left(\frac{c}{b}\right)^5\right] \tag{5}$$

The hydraulic diameter of the channel can be expressed as

$$D_h = \frac{4 \times bc}{2(b+c)} \tag{6}$$

The constant wall temperature Nusselt number can be written as

$$Nu_T = \frac{hD_h}{k_f} \tag{7}$$

From the above equation, the heat transfer coefficient can be found as follows;

$$h_1 = \frac{k_{f_1} Nu_T}{D_h} \tag{8}$$

$$h_2 = \frac{k_{f_2} Nu_T}{D_h} \tag{9}$$

where k_f is the thermal conductivity of the working fluid.

The fin efficiency can be found from the following equations (Equations 14 and 15). The fin efficiency parameters for thin sheet fins are;

$$m_1 = \sqrt{\frac{h_1 2(d_1 + Y)}{k_s d_1 Y}} \tag{10}$$

$$m_2 = \sqrt{\frac{h_2 2(d_2 + Y)}{k_s d_2 Y}} \tag{11}$$

where k_s is the thermal conductivity of the heat exchanger material.

The fin thickness of the hot and the cold flow side is *d*, as shown in the following equations;

$$d_1 \frac{X - [N_1 /(Z/2a + 2b)] \times C}{N_1/(Z/2a + 2b) + 1} \tag{12}$$

$$d_2 \frac{X - [N_2 /(Z/2a + 2b)] \times C}{N_2/(Z/2a + 2b) + 1} \tag{13}$$

Therefore, the fin efficiency is;

$$\eta_{f_1} = \frac{\tanh(m_1 \times b/2)}{m_1 \times b/2} \tag{14}$$

$$\eta_{f_2} = \frac{\tanh(m_2 \times b/2)}{m_2 \times b/2} \tag{15}$$

The total heat transfer area of the hot and the cold flow side is;

$$A_{t_1} = N_1 A_{f_1} + A_{b_1} \tag{16}$$

$$A_{t_2} = N_2 A_{f_2} + A_{b_2} \tag{17}$$

Where the surface area of heat sink is;

$$A_{f_1} = \left(\frac{b}{2}\right) \times 2 \times Y \tag{18}$$

$$A_{f_2} = \left(\frac{b}{2}\right) \times 2 \times Y \tag{19}$$

The mean area of heat sink is;

$$A_{b_1} = N_1 c Y \tag{20}$$

$$A_{b_2} = N_1 c Y \tag{21}$$

Therefore, the overall efficiency of fin array is;

$$\eta_{0_1} = 1 - \frac{N_1 A_{f_1}}{A_{t_1}} (1 - \eta_{f_1}) \tag{22}$$

$$\eta_{0_2} = 1 - \frac{N_2 A_{f_2}}{A_{t_2}} (1 - \eta_{f_2}) \tag{23}$$

The overall thermal conductance ($A_t U$) is;

$$A_t U = \frac{1}{1/\alpha_1 XYZ h_1 \eta_{0_1} + 1/(\alpha_2 XYZ h_2 \eta_{0_2})} \tag{24}$$

$$NTU = \frac{A_t U}{C_{\min}} \tag{25}$$

Where $C_{min} = mc_p$, m is the mass flow rate and the effectiveness of the heat exchanger is;

$$\varepsilon = 1 - \exp[(1/C_r)(NTU)^{0.22}\{\exp\{[-C_r(NTU)^{0.78}] - 1\}] \tag{26}$$

Where $Cr = C_{min}/C_{max}$.

To have come this far, the effectiveness calculations have been established for the heat exchanger pressure drop of the rectangular channel in the heat exchanger. The working fluid in the channels is assumed as a fully developed laminar flow. The Darcy friction factor (Shah and London, 2007) is;

$$f_1 = 96\left[1 - 1.3553\left(\frac{c}{b}\right) + 1.9467\left(\frac{c}{b}\right)^2 - 1.7012\left(\frac{c}{b}\right)^3 + 0.9564\left(\frac{c}{b}\right)^4 - 0.2537\left(\frac{c}{b}\right)^5\right] / R_{e_1} \quad (27)$$

$$f_2 = 96\left[1 - 1.3553\left(\frac{c}{b}\right) + 1.9467\left(\frac{c}{b}\right)^2 - 1.7012\left(\frac{c}{b}\right)^3 + 0.9564\left(\frac{c}{b}\right)^4 - 0.2537\left(\frac{c}{b}\right)^5\right] / R_{e_2} \quad (28)$$

The mass velocity is;

$$G_1 = m_1 / A_{c_1} \quad (29)$$

$$G_2 = m_2 / A_{c_2} \quad (30)$$

Where m is mass flow rate.

Therefore, the pressure drops of the hot and cold flow sides are;

$$\Delta P_1 = \frac{f_1 G_1^2 Y}{D_h (2g_c)\rho_1} \quad (31)$$

$$\Delta P_2 = \frac{f_2 G_2^2 Y}{D_h (2g_c)\rho_2} \quad (32)$$

where $g_c = 1$.

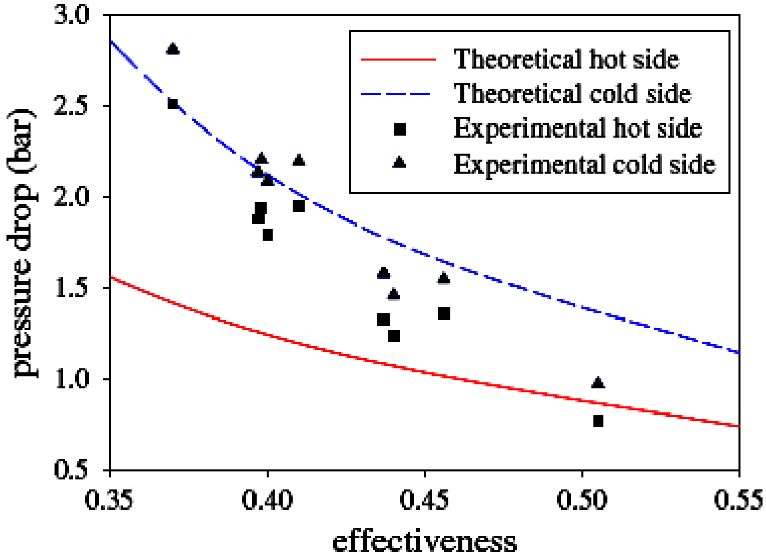

Figure 2: Theoretical and experimental results of pressure drop and effectiveness

The parameters of the dimensions are as expressed in the following (Kang *et al*., 2002); a = 193 µm, b = 200 µm, c = 40 µm, d = 32 µm, X = Y = 9000 µm, Z = 10,218 µm and N = 1625. Total plate number = 26. Channel number of the one layer = 125.

This study used the temperature data from the literature (Kang et al., 2002) substituted for the theoretical equations from above. It can have the outcome value for the heat transfer rate and pressure drop, and the comparison of the theoretical and experimental data is illustrated in Figures 4 and 5. The experimental effectiveness values were between 0.37 and 0.505. The average temperature of the entrance and exit was about 50 ^{0}C. The experimental pressure drop in Figure 2 does not take into account the effects of manifolds by calculation of the loss coefficients for inlet and outlet in manifolds. From Figure 2, the effectiveness increases when the pressure drop reduces. The pressure drop reduces because of the decrease in the working fluid flow rate. At this time, the working fluid has more time to exchange heat, but the ability to carry away heat is less. The flow rate and the heat transfer rate are larger at lower effectiveness. The pressure drop and heat transfer rate of the theoretical and experimental systems show the same trend.

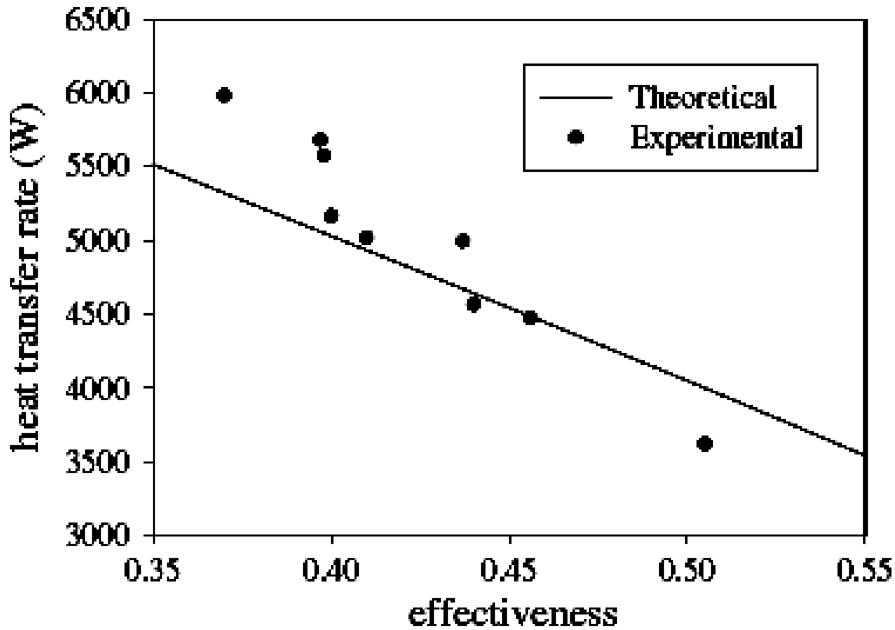

Figure 3: Theoretical and experimental results of the heat transfer rate and effectiveness

Table 1: Temperature parameters and flow rate of the same effectiveness

ε	$T_{h,i}$ (°C)	$T_{h,o}$ (°C)	$T_{c,i}$ (°C)	$T_{c,o}$ (°C)	$\dot{m}_{Si}$ (kg/s)	$\dot{m}_{Cu}$ (kg/s)	T_a (°C)
0.333	40	30	10	20	0.0643	0.0663	25
0.333	50	40	20	30	0.0661	0.0682	35
0.333	60	50	30	40	0.0677	0.0699	45
0.333	70	60	40	50	0.069	0.0713	55
0.333	80	70	50	60	0.07	0.0724	65

Table 2: Temperature parameters and flow rate of the different effectiveness

ε	$T_{h,i}$ (°C)	$T_{h,o}$ (°C)	$T_{c,i}$ (°C)	$T_{c,o}$ (°C)	$\dot{m}_{Si}$ (kg/s)	$\dot{m}_{Cu}$ (kg/s)
0.167	80	70	20	30	0.1746	0.1803
0.333	80	60	20	40	0.0679	0.0701
0.500	80	50	20	50	0.0323	0.0334
0.667	80	40	20	60	0.0139	0.0144
0.833	80	30	20	70	0.0026	0.0027

3. Results and Discussion

After establishing a mathematical model for the micro heat exchanger, the interactive effect between the heat exchanger effectiveness and pressure drop of the working fluid in the micro channels was analyzed. Before calculating, the inflow and the outflow temperature parameters must be established for the same and different effectiveness rates (Tables 1 and 2), where the heat exchanger material parameters used silicon and copper, respectively. From Equation 25, the flow rate m_{Si} and m_{Cu} can be found, and the dimensions are the experimental setting size.

3.1. Same effectiveness, different average temperature

Figures 4 – 5 utilize Table 1 to indicate the relationship between the pressure drop, heat transfer rate and the different average temperature of the hot and cold sides in silicon based micro heat exchanger, and the effectiveness is 0.333. The average temperature is the average value of the entrance and exit fluid temperature of the hot and cold side.

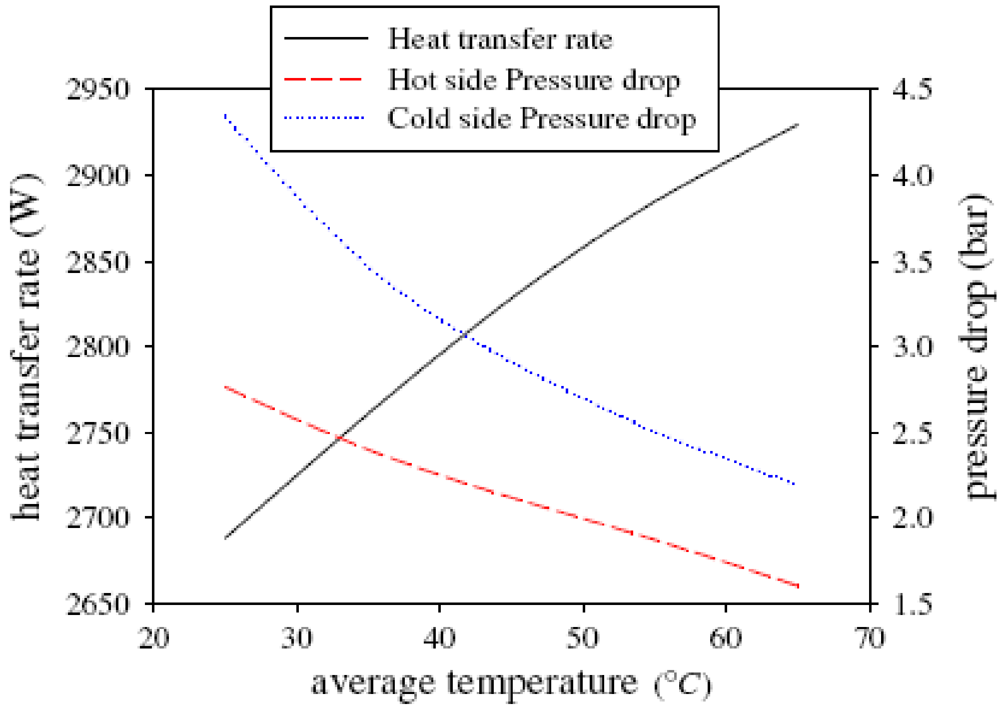

Figure 4: Relationship of the pressure drop and the heat transfer rate in the different average temperature and the effectiveness is 0.333 ($\beta = 10^5/3$)

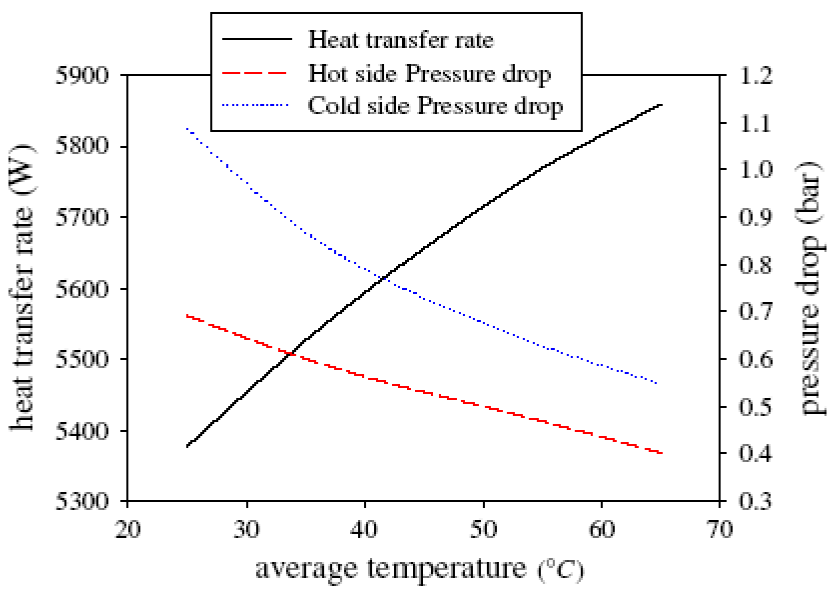

Figure 5: Relationship of the pressure drop and the heat transfer rate in the different average temperature and the effectiveness is 0.333, *X, Y, Z, a, b, c, d* enlarge the double times ($\beta = 10^5/3$).

Heat transfer rate increases because of the increase in the working fluid flow rate. Although the increase of the working fluid flow rate and whole temperature allows the working fluid density to decrease, the inside pressure drop of the micro channels then increases. However, the rising temperature causes the fluid viscosity to decrease and the pressure drop of the heat exchanger then reduces. Under the same flow rate of the hot and cold side channels, the cold side pressure drop is larger than hot side.

In the dimensional effect, the temperature parameters are utilized from Table 1. From Figures 6 and 7, the *X*, *Y*, *Z*, *a*, *b*, *c* and *d* enlarge two times, the density of the heat transfer area β decreases from $10^5/3$ to $10^5/6$, at this time, the pressure drop decreases to 1/4 of the experimental setting. Under the same effectiveness, it can provide the original double heat transfer rate.

From Figure 4, the *X*, *Y*, *Z* enlarge two times, and *a*, *b*, *c* and *d* maintain original size, β also remains $l10^5/3$. The heat transfer rate increases eightfold because of the increase in the total heat transfer area, but at this time, the pressure drop increases four times.

3.2. Different effectiveness, average temperature 50^0C

From Figures 6 and 7, under the same heat transfer rate and effectiveness, enlarging dimension will cause pressure drop to reduce substantially. Overall, the heat transfer rate does not rise very much. When the effectiveness is below 0.4, enlarging dimension has a good suitable range, because the variation in the pressure drop is small.

The influences of enlarging *X*, *Y* and *Z* to the heat exchanger with the same β can be found from comparing Figures 6 and 8. The dimension setting in Figure 8 has a lower pressure drop when the heat transfer rate and effectiveness are the same as shown in Figure 9. Therefore, Figure 8 setting has the higher heat transfer rate and lower pressure drop when the effectiveness is larger than 0.4. From Figure 8, in this dimension condition, it is not suitable for using in the low effectiveness situation. The pressure drop is easily over large. The heat transfer rate increase substantially in the low effectiveness. Contrasting with the experimental setting dimensions, the effectiveness can reach 0.8 and it does not need to reduce the flow rate below 0.002 kg/s.

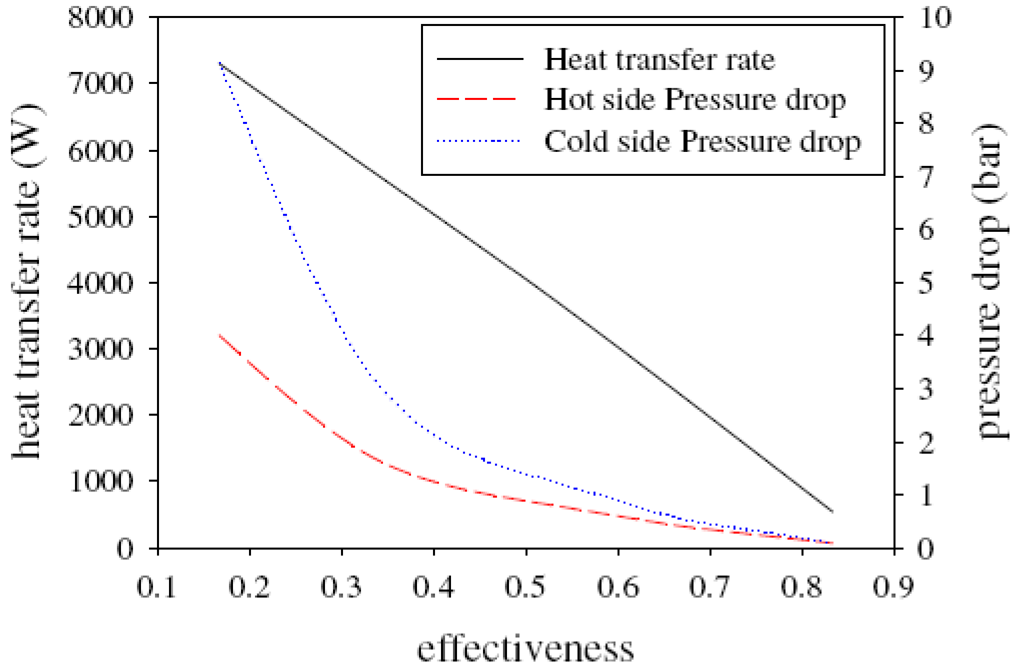

Figure 6: Relationship of the pressure drop and the heat transfer rate in the different effectiveness ($\beta = 10^5/3$)

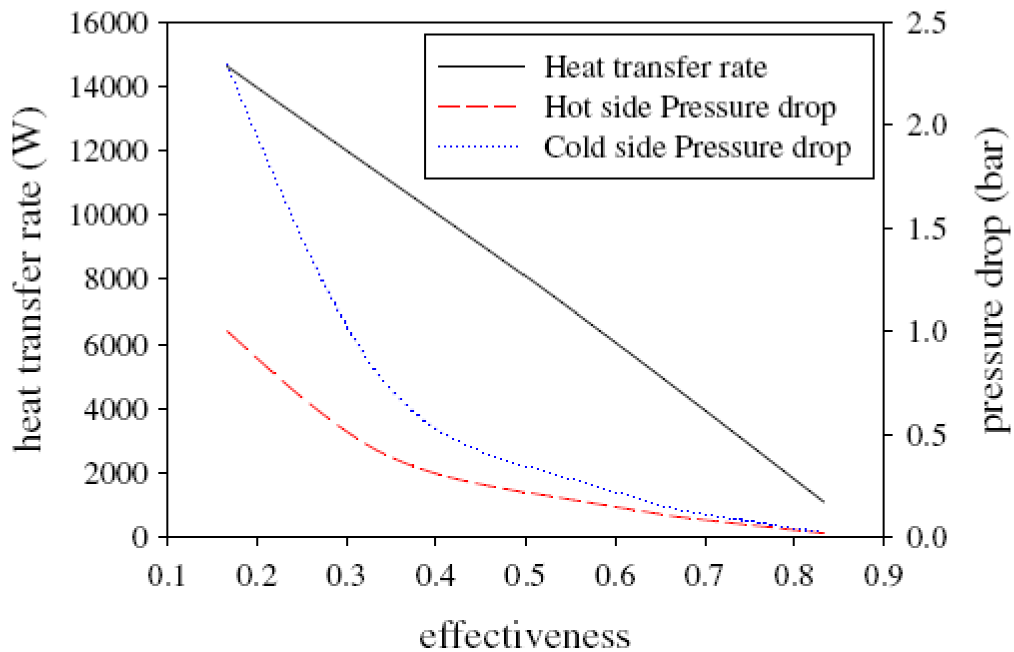

Figure 7: Relationship of the pressure drop and the heat transfer rate in the different effectiveness *X,Y,Z,a,b,c,d* enlarge the double times ($\beta = 10^5/6$)

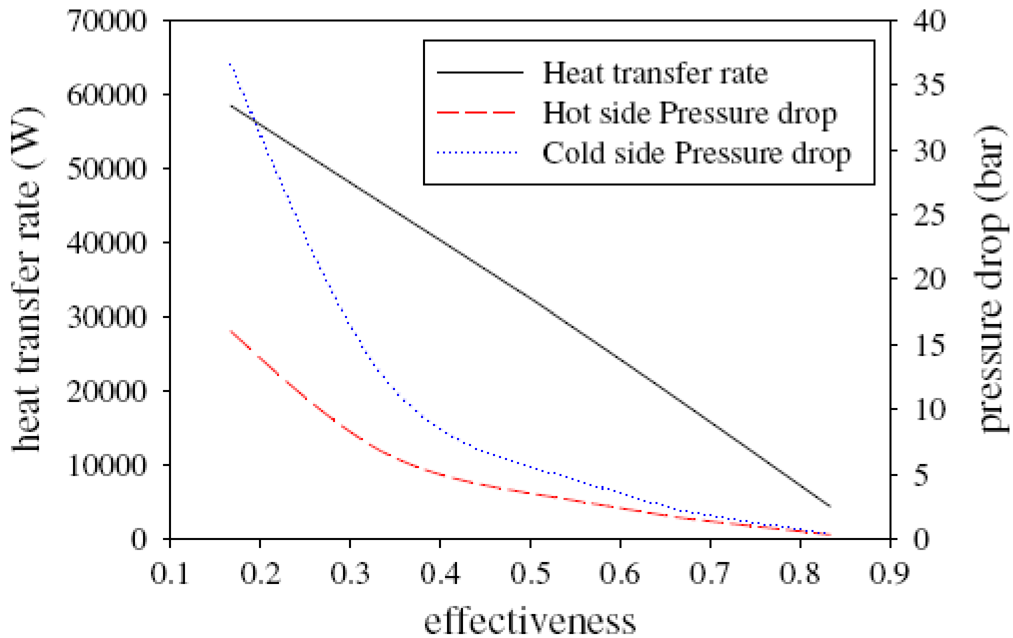

Figure 8: Relationship of the pressure drop and the heat transfer rate in the different effectiveness *X,Y* and *Z*, enlarge the double times and *a,b,c* and *d* is the same ($\beta = 10^5/3$)

4. Conclusion

This study used the fundamental heat transfer and fluid flow equations to establish a theoretical model for a micro heat exchanger in this paper, and it utilized the (11 0) orientation silicon-based micro heat exchanger made using the MEMS fabrication process (Kang *et al*., 2002). The design dimensions and temperature parameters were substituted into the theoretical model to verify the design. This study examined the interactive effect between the effectiveness of the heat exchanger and pressure drop of the micro channels. Key findings from this study are as follows:

(1) Under the same effectiveness, the heat transfer rate increases with rising working fluid temperature in the hot and the cold flow sides. The pressure drop decreases because of the temperature influence, especially on the cold flow side, and the higher average temperature situation has the larger heat transfer rate.

(2) Under the different effectiveness, the heat transfer rate and pressure drop decrease with the increase in effectiveness. Contrasting the increasing magnitude of the pressure drop, the cold flow side is larger than the hot flow side. At this time, the better heat transfer rate is in the low effectiveness situation.

(3) Although the thermal conductivity of the copper (k = 400 W/m K) exceeds that of the silicon (k = 148 W/m k) by more than twice, the influence is very small for a micro

heat exchanger. This is because the fin thickness between the hot and the cold flow channels is very thin, and the thermal resistance of the fin is very small. Therefore, it reduces the influence of the material thermal resistance in the micro heat exchanger.

(4) With the dimensions doubled, there are advantages and disadvantages in the pressure drop and the heat transfer rate.

(5) From comparing Figures 7 and 8, the heat transfer area can increase substantially using the dimension setting in Figure 8, and the characteristics of the heat transfer rate and pressure drop are better than that shown in Figure 7 when the effectiveness is larger than 0.4.

Nomenclature

a	plate thickness
A_b	mean area of heat sink
A_c	free flow area of one side
A_f	surface area of heat sink
A_t	heat exchanger total heat transfer area on one side
b	spacing between plates
c	micro channels width
c_p	specific heat at constant pressure
C_r	capacity-rate ratio
d	fin thickness
D_h	hydraulic diameter
f	friction factor
G	mass velocity
g_c	gravitational constant
h	convention heat transfer coefficient
k	thermal conductivity
m	fin efficiency parameter
$\dot{m}$	mass flow rate
N	total number of channels on one side
NTU	number of transfer units
Nu_T	constant wall temperature Nusselt number
P	pressure
Re	Reynolds number
T	temperature
U	overall heat transfer coefficient
X,Y,Z	principal dimensions of heat exchanger

Greek letters

α	ratio of total heat transfer area on one side of the exchanger to total volume of the exchanger
β	ratio of total transfer area on one side of the exchanger to the volume between the plates of that side

Δ	denotes difference
ε	exchanger effectiveness
η_f	fin efficiency
η_o	overall efficiency of fin array
ρ	mass density

References

Friedrich, C.R. and S.W. Kang (1994). Micro heat exchangers fabricated by diamond machining, *Precision Engineering* **16** 56–59.

Kang,S.W.; Y.T. Chang and G.S. Chang (2002). The manufacture and test of (110) orientation silicon based micro heat exchanger. *Tamkang Journal of Science and Engineering*. 5 (**3**). 129–136.

Kays, W.M. and A.L. London (2004). *Compact Heat Exchanger.* Third ed., McGraw Hill Co., NY, USA, 2004.

Shah, R.K. and A.L. London (2007). *Laminar Flow Forced Convection in Ducts*. Academic Press, London.

Tuckerman, D.B. (1984). *Heat-Transfer Micro-structures for Integrated Circuits*. Ph.D. Thesis, Department of Electronic Engineering, Stanford University, USA.